Journal of Magnetism and Magnetic Materials 482 (2019) 292–295

Contents lists available at ScienceDirect

Journal of Magnetism and Magnetic Materials

journal homepage: www.elsevier.com/locate/jmmm

Research articles

Permalloy-based magnetoplasmonic crystals for sensor applications

V.K. Belyaev[a,*], D.V. Murzin[a], N.N. Perova[a], A.A. Grunin[b], A.A. Fedyanin[b], V.V. Rodionova[a,c]

[a] Institute of Physics, Mathematics and Informational Technologies, Immanuel Kant Baltic Federal University, Kaliningrad 236041, Russia
[b] Faculty of Physics, Lomonosov Moscow State University, Moscow 119991, Russia
[c] National University of Science and Technology MISiS, Moscow 119049, Russia

ARTICLE INFO

Keywords:
Magneto-optical effects
Surface plasmon polaritons
Magnetic field sensor
Magnetioplasmonic crystals

ABSTRACT

This work demonstrates a possibility of creating a magnetic field sensor based on magnetoplasmonic crystal with permalloy layer. Experimental results show that sensitivity of such sensors strongly correlates with the magnetic properties of magnetoplasmonic crystals and slightly depends on the value of transverse magneto-optical Kerr effect. The achieved sensitivity to DC magnetic field at local area of 1 mm^2 was found to be 10^{-6} Oe in modulating field of 5 Oe.

1. Introduction

The simultaneous realization of high sensitivity and locality of a magnetic field sensor is essential in biomedical applications, for example, in magnetocardiography [1,2] and magnetotomography [3]. The required sensitivity for listed applications is about 10^{-6} Oe that can be achieved in sensors exploiting different effects. The main disadvantage of existing sensors is low sensitivity to magnetic field for measurements in small volumes [4,5]. One of the possible ways to design the magnetic field sensor with high locality is using of plasmon assisted magneto-optical effects [6–9]. In this case, magneto-optical effects are enhanced by the excitation of surface plasmon polaritons (SPPs) – combined excitations of surface plasmons on the metal/dielectric interface and photons of incident light that leads to localization of incident light energy in proximity of the surface [10–12].

Enhancement of magneto-optical effects through the excitation of SPP can be achieved by the use of the magnetoplasmonic crystals (MPlCs) made of ferromagnetic metal deposited on one-dimensional subwavelength gratings [13–16]. In such systems transverse magneto-optical Kerr effect (TMOKE), which allows one to control the intensity of the reflected p-polarized light, can be enhanced by the excitation of SPPs applying the diffraction method [17]. That leads to appearance of narrow asymmetrical Fano-shape resonances [18,19].

The achieved sensitivity of DC magnetic field sensor based on MPlCs is 10^{-5} Oe at 2 mm^2 area of measurements in modulating field of 13 Oe [20]. These values are matched to required characteristics of sensors for biomedical applications [21]. The use of AC magnetic field is necessary condition to detect a low DC magnetic field for the sensors based on MPlCs.

There are several ways on further improving the MPlC-based sensor's overall design: (i) amplification of TMOKE value in a narrow spectral range by varying the magnetic and magneto-optical properties through the changes the substrate shape/parameters, (ii) noise reduction and (iii) decrease of controllable AC magnetic field by choosing a composition of MPlCs for the reducing of the saturation field. This work devotes to study of magneto-optical and optical properties of MPlCs with permalloy layer, perspective to reach the goal (iii). The factors affecting the sensitivity to DC magnetic field are considered.

2. Materials and methods

MPlCs were made by DC magnetron sputtering of permalloy $Ni_{80}Fe_{20}$ (Py) target onto the polymer substrates, Sub_2 and Sub_3, with one-dimensional quasi-sinusoidal gratings. Sub_2 and Sub_3 have following parameters: periods are $d_2 = 320$ nm and $d_3 = 740$ nm, profile heights are $h_2 = 20$ nm and $h_3 = 100$ nm. Thicknesses of Py were chosen as 100 nm and 130 nm. For each composition, reference samples on smooth silicon substrates (Sub_1) were fabricated in the same fabrication cycles. Spatial profiles and thicknesses of Py layer of fabricated samples were attested by atomic force microscopy technique (AFM).

Optical and magneto-optical properties of fabricated samples were investigated by using the experimental setup consisted of halogen lamp serving as the light source, Glan-Taylor prism (GT) as the polarizer, pair of electromagnets (Helmholtz coils), a monochromator with a photomultiplier tube (PMT) and Lock-In amplifier as a detecting system. Reflectivity spectra were measured by modulation of the light beam with an optomechanical chopper at frequency of 235 Hz and TMOKE spectra were measured in saturating external AC magnetic field with

* Corresponding author.
E-mail addresses: belyaev@lnmm.ru, vbelyaev@kantiana.ru (V.K. Belyaev).

https://doi.org/10.1016/j.jmmm.2019.03.052
Received 31 August 2018; Received in revised form 13 January 2019; Accepted 8 March 2019
Available online 09 March 2019
0304-8853/

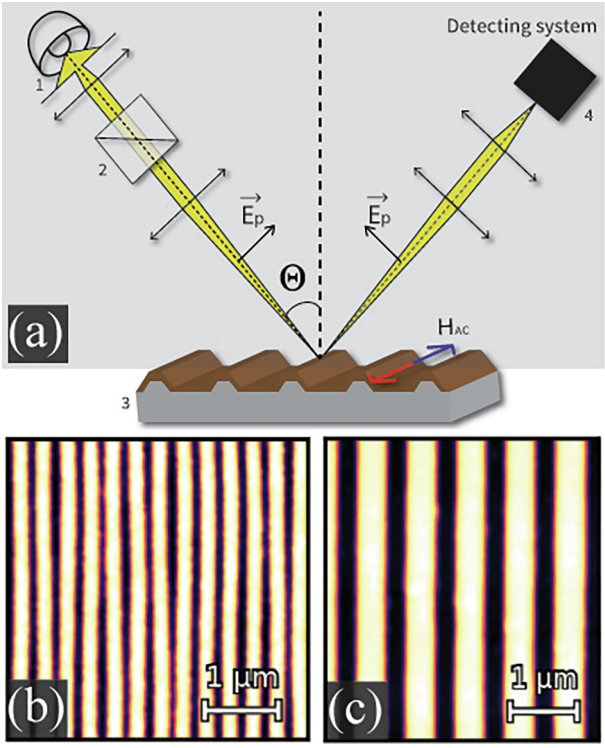

Fig. 1. Panel (a): Schematic view of the setup, where: 1 – light source; 2 – GT; 3 – MPlC; 4 – detecting system; θ is the angle of incidence. Panels (b) and (c): surfaces profiles obtained by AFM for the MPlCs based on Sub_2 and Sub_3, respectively.

the magnitude of 100 Oe, oscillating at the frequency of 67 Hz. Light beam was focused into the spot of 1 mm^2. To observe the maximum of TMOKE the incidence angle, θ, was chosen as 68° [22]. Principal scheme of the experimental setup and AFM images of MPlCs surfaces based on Sub_2 and Sub_3 are shown in Fig. 1.

For each sample, spectral dependences of the reflectivity in absence of external magnetic field, R_0, and in saturation AC field with the magnitude of 100 Oe, ΔR, were measured. TMOKE value was calculated according to the formula: $\delta(\lambda) = (R_{+H} - R_{-H})/R_0 = \Delta R/R_0$, where R_{+H} and R_{-H} denote the field dependent reflection amplitudes.

To estimate the dependences of magneto-optical response to weak external magnetic field, dependences of ΔR(H) on external AC magnetic field at the resonance wavelength, corresponding to the maximum of TMOKE signal, were measured. Signal-to-noise ratio, SNR_{AC}, was calculated according to the formula: $SNR_{AC} = \Delta R(H)/\sigma$, where $\sigma = \sqrt{\sum_0^N (\Delta R_N - \overline{\Delta R})^2/(N-1)}$ is standard deviation of noise measured at the same wavelength in saturation magnetic field for $N = 500$ acquisition points.

Sensitivity was calculated as the ratio of the magnetic field range, ΔH_{AC}, to the difference of SNR_{AC} values in selected ΔH_{AC} ranges, ΔSNR_{AC}. The selected ΔH_{AC} range corresponds to the region of full width at half maximum of the $\partial SNR_{AC}/\partial H_{AC}$.

3. Results and discussions

Reflectivity and TMOKE spectra for all samples are shown in Fig. 2. Samples based on smooth silicon substrates show no enhancement of TMOKE value and can be used as reference. Clearly observable minimums of the specular reflectivity for the MPlCs based on Sub_2 and Sub_3 represent -1st and -2nd orders of diffraction, respectively, and correspond to fulfilment of phase-matching conditions between wavevectors of incident light and SPPs. It can be written as follows: $\boldsymbol{k}_{SPP} = \boldsymbol{k}_x + n\boldsymbol{g}$, where $\boldsymbol{k}_{SPP}$ and $\boldsymbol{k}_x$ are SPPs wavevectors and projection of the incident radiation wavevector onto metal surface, $\boldsymbol{g}$ is a reciprocal vector and n is an integer.

The diffraction scheme used for SPPs excitation allowed one to observe 35.4 and 54.3 times magnification of TMOKE values at resonant wavelengths for MPlCs based on Sub_2 and Sub_3 in comparison with Sub_1, respectively.

MPlCs based on Sub_2 have lower reflectivity and higher values of TMOKE enhancement that can be explained in terms of different values of relative diffraction efficiency ε_a. The ε_a value is the ratio of the light flux at a given wavelength, diffracted into a given diffraction order, to the total light flux reflected by grating [23] that can be controlled by the changes of grating profile shape and the parameters of the grating like the period and stripe height. Increase of the ε_a value leads to strengthen the coupling of plasmon oscillations and diffracted light caused by increased height of the stripes on the surface of the Sub_2 [22].

Fig. 3 shows the SNR_{AC} dependences for the studied samples. It was shown that the shape of field dependent magneto-optical response correlates with the relative changes in magnetic moment of ferromagnetic layer.

Shape of field dependent magneto-optical response is determined by magnetic properties of MPlCs. Magnetic properties of Py based MPlCs can be tuned by changing the ferromagnetic layer thickness and substrate parameters d and h [24]. Increase of mentioned parameters causes the growth of the necessary saturation field and ΔH_{AC} region. Thus, comparing the MPlCs based on Sub_2 and Sub_3: Sub_2 allows one to get steeper dependence of SNR_{AC} at low magnitudes of modulating field while Sub_2 allows one to expand the measurable field region. The sensitivity mostly depends on shape of field dependent magneto-optical response and weakly correlates with the values of $\Delta\delta$, which can be clearly seen in Figs. 2 and 3.

Table 1 represents the summarized results on MPlCs investigation, where the values of TMOKE at a narrow spectral range $\Delta\delta$, spectral width of the TMOKE resonance $\Delta\lambda_{res}$ and the measurable field region ΔH_{AC} are graphically defined on the corresponding figures.

The sensitivity of the sensor based on Py MPlC is comparable with the sensor based on silver/iron magnetoplasmonic crystals. As an advantage, the value of modulating field is three times lower than for the sensor based on silver/iron magnetoplasmonic crystal [20].

4. Conclusions

Optical and magneto-optical properties of MPlCs based on one-dimensional diffraction gratings with different parameters were studied. Possibility to use permalloy-based MPlCs as highly sensitive sensors of magnetic field is represented in the article. Measured field dependences of SNR on magnitude of external AC magnetic field allowed one to calculate the sensitivity and to denote measurable field region with maximum sensitivity for the sensors based on MPlCs. Possibility to reduce the magnitude of modulating AC field by changing the permalloy thickness, substrate grating period and height was found.

Optimal characteristics for the magnetic field sensor based on MPlC with permalloy layer are found to be for permalloy thickness of 100 nm and one-dimensional diffraction grating with period and height equal to 320 nm and 20 nm, respectively. The achieved sensitivity is 4.4 μOe with spot size of 1 mm^2 in modulating AC field of 5.3 Oe.

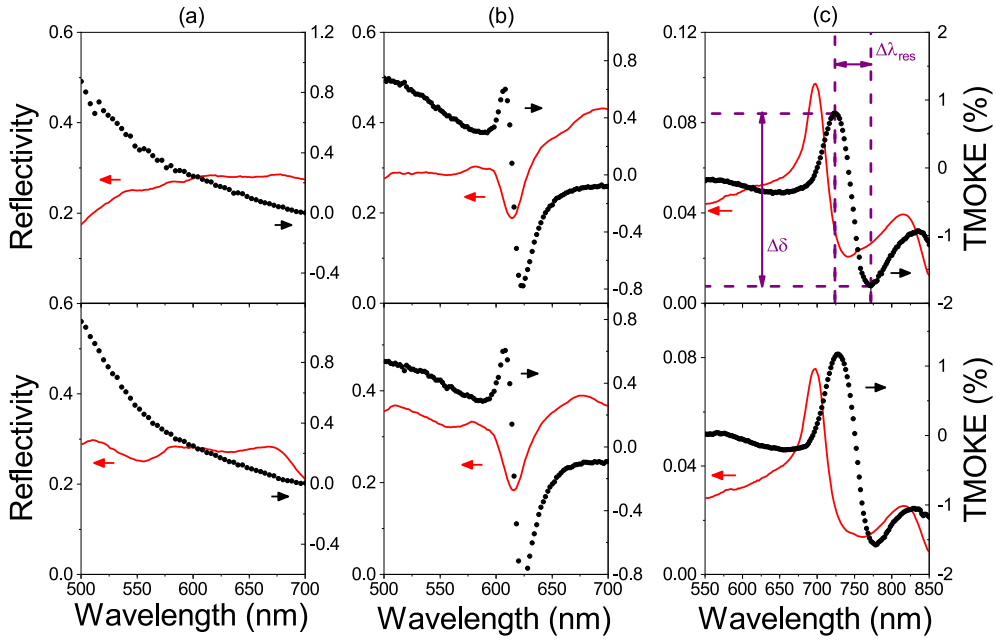

Fig. 2. Reflectivity ($R(\lambda)$, red solid curve) and TMOKE ($\delta(\lambda)$, black circles) spectra for the studied samples. First and second rows represent spectra for the samples with Py thicknesses of 100 nm and 130 nm, respectively. Columns (a), (b) and (c) represent spectra for the samples based on Sub_1, Sub_2 and Sub_3, respectively. Purple lines and dash lines define the values of TMOKE at a narrow spectral range $\Delta\delta$ and spectral width of the TMOKE resonance $\Delta\lambda_{res}$. (For interpretation of the references to colour in this figure legend, the reader is referred to the web version of this article.)

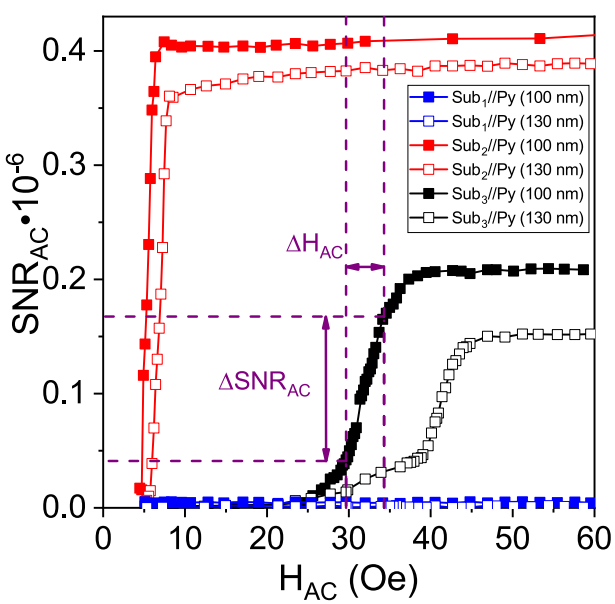

Fig. 3. SNR_{AC} dependences for studied samples. Blue, red and black rectangles denote SNR_{AC} for the samples based on Sub_1, Sub_2 and Sub_3, respectively. Solid and empty symbols represent data obtained for the samples with Py thicknesses of 100 nm and 130 nm, respectively. Purple lines and dash lines define the values of magnetic field range, ΔH_{AC}, and the difference of signal-to-noise ratio in selected ΔH_{AC} range - ΔSNR_{AC}. (For interpretation of the references to colour in this figure legend, the reader is referred to the web version of this article.)

Table 1
Measured and calculated parameters of MPlCs, where $\Delta\delta$ – value of TMOKE at a narrow spectral range; $\Delta\lambda_{res}$ - spectral width of the TMOKE resonance; ΔH_{AC} – measurable field region.

Substrate	Permalloy layer thickness, nm	$\Delta\delta$,%	$\Delta\lambda_{res}$, nm	ΔH_{AC}, Oe	Sensitivity, μOe
Sub_2	100	1.4	14	1.3	4. 4
Sub_3		2.6	48	4.6	38
Sub_2	130	1.5	16	1.5	6. 0
Sub_3		2.8	50	13.6	90

Acknowledgments

VKB acknowledges 5 top 100 Russian Academic Excellence Project at the Immanuel Kant Baltic Federal University. VVR acknowledges the Russian Ministry of Science and Education for financial support in the framework of Government assignment 3.9002.2017/6.7. AAG and AAF acknowledge the MSU Quantum Technology Center and Russian Minustry of Science and Education (#14.W03.31.0008) for partial support.

References

[1] K. Tsukada, Y. Haruta, T. Mitsui, et al., Multichannel SQUID system detecting tangential components of the cardiac magnetic field, Rev. Sci. Instrum. 66 (1995) 5085.
[2] H. Koch, Recent advances in magnetocardiography, J. Electrocardiol. 37 (2004) 117.
[3] L. Marmugi, F. Renzoni, Optical Magnetic Induction Tomography of the Heart, Sci. Rep. 6 (2016) 23962.
[4] P. Ripka, M. Janosek, Advances in magnetic field sensors, IEEE Sens. J. 10 (2010) 1108.
[5] Yu.E. Grigorashvili, L.P. Ichkitidze, N.N. Volik, Magnetomodulation sensor of a weak magnetic field based on HTS (Bi, Pb) 2Sr 2Ca 2Cu 3O x ceramics, Phys. C 435 (2006) 140.
[6] Y. Souche, V. Novosad, B. Pannetier, O. Geoffroy, Magneto-optical diffraction and transverse Kerr effect, J. Magn. Magn. Mater. 177–181 (1998) 1277–1278.
[7] N. Maccaferri, X. Inchausti, A. García-Martín, J.C. Cuevas, D. Tripathy, O. Adeyeye, P. Vavassori, Resonant enhancement of magneto-optical activity induced by surface plasmon polariton modes coupling in 2D magnetoplasmonic crystals, ACS Photon. 2 (2015) 1769–1779.
[8] L. Ming, Z. Xiang, Plasmon-boosted magneto-optics, Nat. Photon. 7 (2013) 429–430.
[9] V. Safarov, V. Kolsobukin, C. Hermann, G. Lampel, J. Peretti, Magneto-optical effects enhanced by surface plasmons in metallic multilayer films, Phys. Rev. Lett. 73 (1994) 3584.
[10] A. Zayats, I. Smolyaninov, Near-field photonics: surface plasmon polaritons and localized surface plasmons, J. Opt. A: Pure Appl. Opt. 5 (2003) 1650.
[11] N. Bonod, R. Reinisch, E. Popov, M. Neviere, Optimization of surface-plasmon-enhanced magneto-optical effects, J. Opt. Soc. Am. B 21 (2004) 791.
[12] G. Armelles, A. Cebollada, A. García-Martín, M.U. González, Magnetoplasmonics: combining magnetic and plasmonic functionalities, Adv. Opt. Mater. 1 (2013) 10–35.
[13] Y. Souche, A. Tufaile, C. Santi, V. Novosad, A. Santos, Figure of merit for transverse

magneto-optical Kerr effect, J. Magn. Magn. Mater. 226–230 (2001) 1686–1687.
[14] A. Grunin, A. Zhdanov, A. Ezhov, E. Ganshina, A. Fedyanin, Surface-plasmons-induced enhancement of magneto-optical Kerr effect in all-nickel subwavelength nanogratings, Appl. Phys. Lett. 97 (2010) 261908.
[15] G.S. Krinchik, E.E. Chepurova, T.I. Kraeva, Excitation of magnetized-plasma surface waves in nickel, JETP Lett. 40 (1984) 776.
[16] J. Jose, F. Segerink, J. Korterik, A. Gomez-Casado, J. Huskens, J. Herek, H. Offerhaus, Enhanced surface plasmon polariton propagation length using a buried metal grating, J. Appl. Phys. 109 (2011) 064906.
[17] P. Karpinski, A. Miniewicz, Surface plasmon polariton excitation in metallic layer via surface relief gratings in photoactive polymer studied by the finite-difference time-domain method, Plasmonics 6 (2011) 541.
[18] N. Kostylev, I. Maksymov, J. Williams, et al., Plasmon-assisted high reflectivity and strong magneto-optical Kerr effect in permalloy gratings, Appl. Phys. Lett. vol., 102, (2013) 121907.
[19] B. Diaz-Valencia, J. Mejía-Salazar, N. Oliveira, N. Porras-Montenegro, Pablo Albella, Enhanced transverse magneto-optical kerr effect in magneto-plasmonic crystals for the design of highly sensitive plasmonic (bio)sensing platforms, ACS Omega 2 (2017) 7682.
[20] V. Belyaev, A. Grunin, A. Fedyanin, V. Rodionova, AC and DC magnetic field sensor based on magnetoplasmonic crystal, MISM17 book of abstracts, 2017, p. 192.
[21] L. Panina, Electromagnetic sensor technology for biomedical applications, Int. J. Integr. Med. (2011) 215–217.
[22] A. Grunin, A. Chetvertukhin, T. Dolgova, A. Ezhov, A.A. Fedyanin, Magnetoplasmonic crystals based on commercial digital discs, J. Appl. Phys. 113 (2013) 17A946.
[23] C. Palmer, E. Loewen, Diffraction grating handbook, Newport Corp. 9 (2005) 128.
[24] V.K. Belyaev, V.V. Rodionova, A.G. Kozlov, A.V. Ognev, A.S. Samardak, Magnetic properties and geometry driven magnetic anisotropy of magnetoplasmonic crystals, J. Magn. Magn. Mater. 480 (2019) 150–153.